Received December 8, 2018, accepted December 28, 2018, date of publication January 1, 2019, date of current version February 20, 2019.

Digital Object Identifier 10.1109/ACCESS.2018.2890555

A Full-Freedom Wireless Power Transfer for Spheroid Joints

ZHONGYU DAI, (Student Member, IEEE), JUNHUA WANG, (Member, IEEE), LEI JIN, HANG JING, ZHIJIAN FANG, (Member, IEEE), AND HAOLI HOU, (Member, IEEE)
School of Electrical Engineering and Automation, Wuhan University, Wuhan, China

Corresponding author: Junhua Wang (junhuawang@whu.edu.cn)

This work was supported in part by the National Natural Science Foundation of China under Grant 51707138 and Grant 51507114, and in part by the National Key Research and Development Plan under Grant 2017YFB1201002.

ABSTRACT A full-freedom wireless power transfer for spheroid joints is proposed to solve the problem of power transmission between the caput-articularis and the acetabulum in a spheroid joint. According to the characteristics of the spheroid joint, a hemispherical coil and a spherical coil are designed having no effect on the performance of the joint. Hemispherical and spherical magnetic cores are used to optimize the magnetic field distribution of the transmitter and receiver coils to reduce the electromagnetic influence on the external environment of the acetabulum and the internal environment of the caput-articularis during the power transmission process. Practical results obtained from a hardware prototype are included. They confirm that the maximum transmission efficiency of the designed system is 91%, and the transmission efficiency is always higher than 80% when the caput-articularis rotates freely.

INDEX TERMS Spheroid joints, full-freedom, hemispherical coils, spherical coil, wireless power transfer (WPT).

I. INTRODUCTION

The wireless power transfer (WPT) technology can perform non-contact power transmission with the electromagnetic field as a medium [1]–[3]. This has many significant advantages: 1) overcoming the inherent defects of wire media, 2) improving the safety of power transmission, and 3) increasing the flexibility of electrical equipment [4]. In recent years, it has become a hot topic in the field of engineering applications, and has been widely used in many fields, such as implant equipment, robots, unmanned aerial vehicles, electric vehicles, etc. [2], [3], [5], [6].

The WPT structures used in different fields are varied. The most common form is the directional WPT structure, composed of two spiral coils or helix coils. In this structure, relay coils are often used to increase the transmission distance, and magnetic cores are added for the enhancement of the transmission efficiency [7], [8]. They are shown in Fig. 1. Directional WPT is mainly used for directional power supply of a single device. It has the advantages of high transmission efficiency and long transmission distance. However, with the increase of electrical equipment, many devices will be installed in a limited space. To meet the power need of many electrical equipment at the same time, a one-to-many WPT structure was proposed [4], [9]–[11], as shown in Fig. 2. Fig. 2(a) shows a 2D planar, one-to-many WPT structure [9]. In the plane, the devices can be wirelessly charged at the same time. Fig. 2 (b) shows a one-to-many form in three dimensional space, which can satisfy the simultaneous power supply for a number of devices at any location [4], [10]. There is also a kind of WPT structures designed for special situations, as shown in Fig. 3 [12]–[14]. Fig. 3 (a) shows a bowl-shaped coil structure that can achieve a uniform magnetic field distribution in the limited space inside the coil. It can provide power for portable devices regardless where they are located in the bowl-shaped coil. Another structure is a coaxial coil shown in Fig. 3 (b). The transmitter and receiver coils are coaxial, but with different radii. It is mainly used for wireless energy transmission at the rotating shaft.

A large number of different WPT structures have been studied, but few researchers have focused on the WPT structure for spheroid joint [15], [16]. The spheroid joint composed of two parts is a synovial joint, and it is the most flexible joint. The movable end is a ball (the caput-articularis) that can be inserted into the groove of the fixed end (the acetabulum). The caput-articularis can be rotated and turned in all directions. Many joints of the human body are spheroid

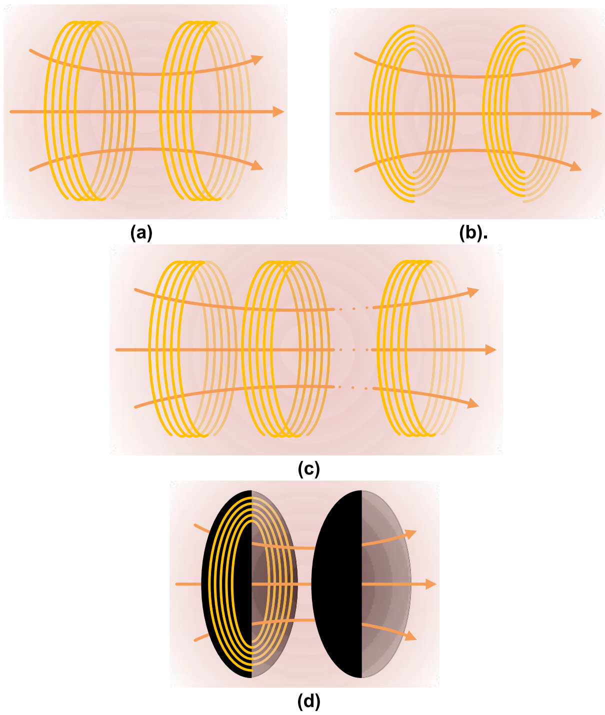

FIGURE 1. Directional WPT. (a) spiral coil. (b) helix coil. (c) WPT with relay coils. (d) WPT with magnetic cores.

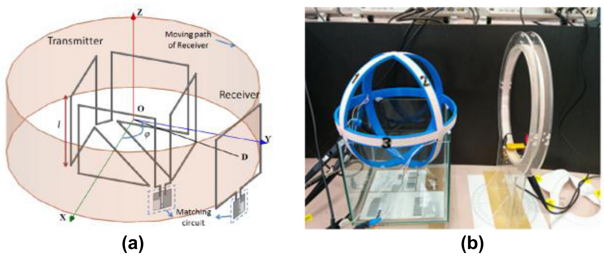

FIGURE 2. Omnidirectional WPT. (a) A 2D planar WPT [9]. (b) A 3D WPT [10].

joint to ensure the flexibility of the human body movement. Fig. 4 (a) shows one spheroid joint of human which is the hip joint. Spheroid joints are also widely used in the industry to increase the flexibility of the connection, such as camera base, piston and so on, as shown in Fig. 4 (b). In industrial applications, power is usually transmitted between the caput-articularis and the acetabulum, and the wire is the most common medium for the power transfer. If the wire is laid along the surface of a spheroid joint, it needs to reserve enough length to ensure the flexibility of the spheroid joint. In theory, only when the reserved wire is infinitely long can the flexibility of joint rotation be guaranteed. This will lead to waste of wires and other problems. If power is transmitted through the caput-articularis and the acetabulum, the reserved wire can be shortened. However, due to the high flexibility of the spheroid joint, the internal wires are often twisted and bent, which will greatly reduce the life of the wires, accelerate the insulation loss of the wires, and even lead to electric leakage accidents.

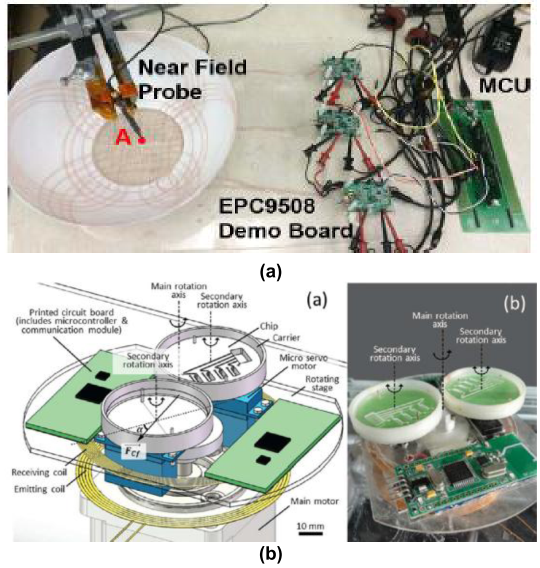

FIGURE 3. WPT structures tailored for special use environments. (a) The bowl-shaped coil [13]. (b) The coaxial structure coil [14].

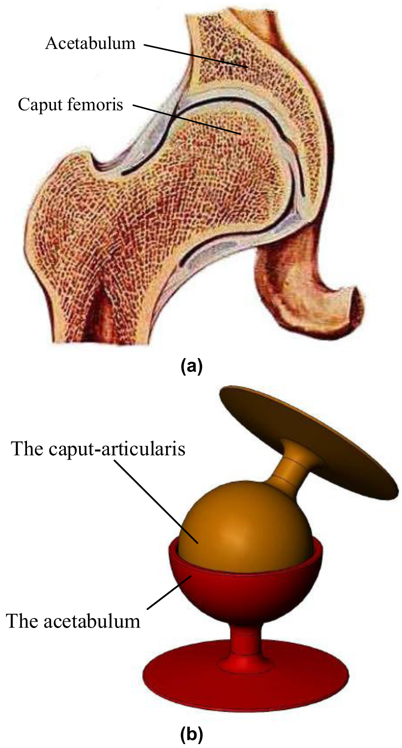

FIGURE 4. A spheroid joint and its application. (a) The hip joint. (b) The spheroid joint.

In this paper, based on the non-contact power transmission characteristics of WPT and the requirements of the spheroid joint power transmission, a full-freedom WPT system suitable for spheroid joint is proposed. The WPT coils are embedded in the caput-articularis and the acetabulum. The receiver coil is approximately spherical. It can make sure that the caput-articularis receives power wherever it

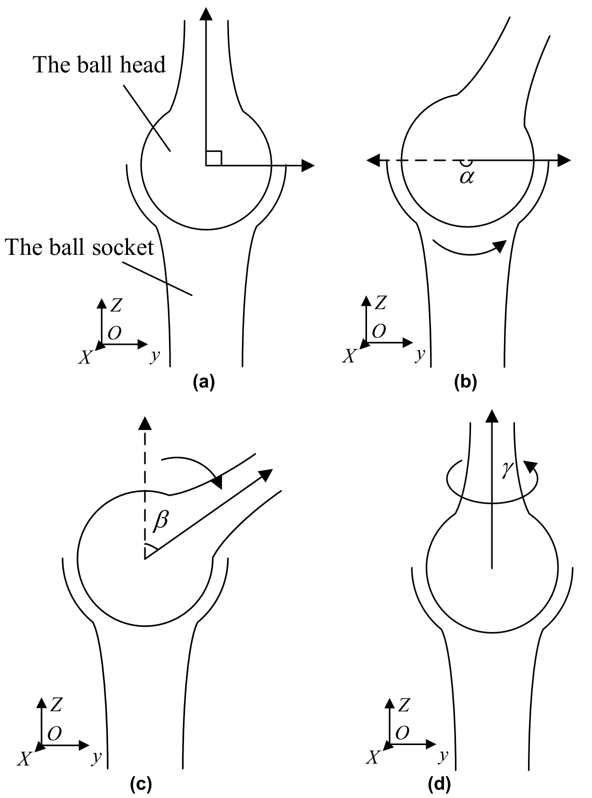

FIGURE 5. WPT structures tailored for special use environments.

rotates to. In order to increase the area of the transmitter coil and improve the transmission efficiency, the acetabulum coil is designed to be hemispherical.

II. THE WPT STRUCTURE OF THE SPHEROID JOINT

A. THE CHARACTERISTICS OF THE SPHEROID JOINT AND THE REQUIREMENT OF THE COIL

The spheroid joint is highly flexible and can rotate in all directions, as shown in Fig. 5. It has some unique features in its rotation.

1) The acetabulum is an approximate hemisphere, and the area of its package is lightly greater than that of a hemisphere. That is, the angle α from one point of the ball-and-socket section (YOZ plane) to another point is about 180°, as shown in Fig. 5(b).
2) The caput-articularis can freely rotate in the vertical direction (that is, the X-axis or Y-axis is used as the rotation axis). The swing angle is not more than 60°, that is $\beta \leq 60°$, as shown in Fig. 5(c).
3) The caput-articularis can also rotate in the horizontal plane (that is, the Z axis is used as the rotation axis) without any angle limiting. That is $\gamma = 360°$, as shown in Fig. 5 (d).

The full-freedom WPT for spheroid joint cannot change its original structure. The performances also cannot be affected, including its flexibility, the internal environment of the caput-articularis and the external environment of the acetabulum. So the receiver coil and the transmitter coil of the spheroid joint must have the following characteristics:

1) The transmitter coil will be implanted in the acetabulum and cannot change the original shape of the acetabulum. The coverage area of the transmitter coil is as large as possible to increase the transmission efficiency. Therefore, a hemispherical coil with a section rotation angle $\alpha' \leq \alpha$ is designed for the transmitter as shown in Fig. 6 (a);

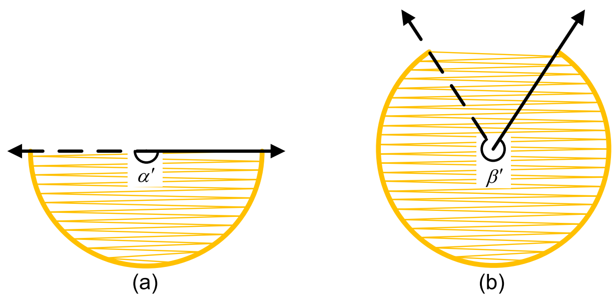

FIGURE 6. The coils for the spheroid joint. (a) The transmitter coil. (b) The receiver coil.

2) The receiver coil also cannot make effect on the shape of the caput-articularis. Additionally, it must ensure that the caput-articularis swings to any position in the vertical direction (the X-axis or Y-axis is used as the center axis) can receive enough power. So the spherical coil is the best choice, and it can be embedded in ball head. The coil needs to meet the section rotation angle $\beta' \geq 2\beta + 180°$, as shown in Fig. 6 (b);
3) When the caput-articularis rotates in the horizontal plane (that is, the Z axis is used as the rotation axis), the WPT must ensure the efficiency and the stability of power transfer, and reduce the influence of electromagnetic field. The magnetic field distribution inside the transmitting coil should be as uniform as possible, and it inside the caput-articularis and outside the spheroid joint are supposed to be as small as possible.

B. THE COILS FOR THE SPHEROID JOINT

There are two ways for the coils to be made when its outline characteristics are determined. One is that the adjacent turns of the coils are equal in pitch, and the other is that the adjacent turns of the coils are equal in vertical height. Fig. 7 shows the models of the coils coiled built in different ways.

Magnetic fields have a certain impact on human tissues and other electronic devices [17], [18]. In order to reduce this influence on human tissues and the surrounding environment, and improve the transmission efficiency, the coils are usually optimized by adding magnetic cores. The Transmitter coil of the spheroid joint needs to focus the magnetic field within the coil as much as possible for the receiver coil to receive, while reduces its impact on the surrounding environment. So the magnetic core of the transmitter coil is also a hemisphere, and installed outside the coil, as shown in Fig. 8(a). The magnetic

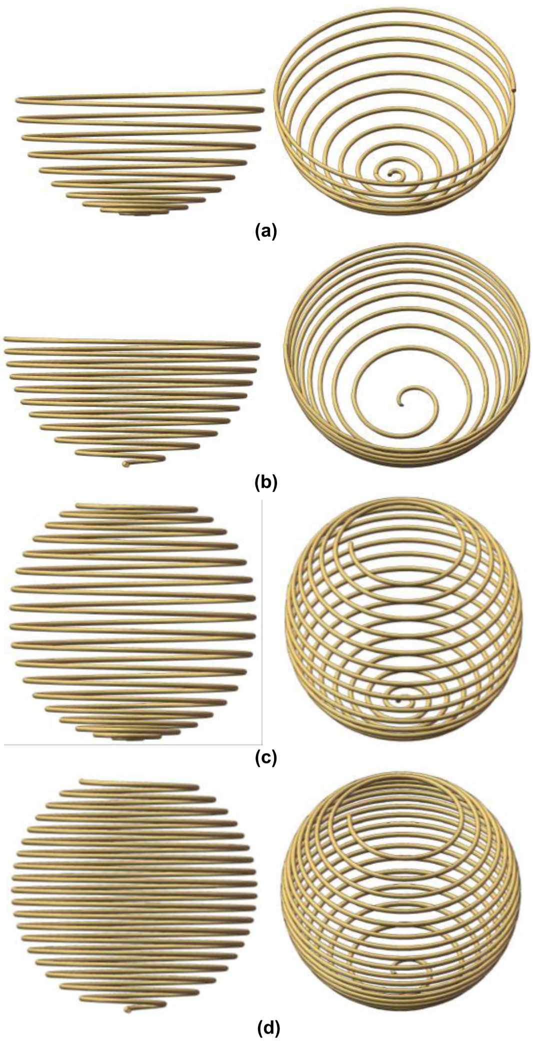

FIGURE 7. The coils coiled in two ways. (a) The transmitter coil with equal pitch between adjacent turns; (b) The transmitter coil with equal spacing between adjacent turns in vertical height; (c) The receiver coil with equal pitch between adjacent turns; (d) The receiver coil with equal spacing between adjacent turns in vertical height.

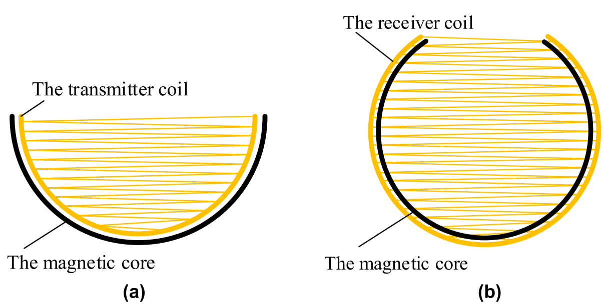

FIGURE 8. The coils with magnetic cores. (a) The transmitter coil with the outer magnetic core. (b) The receiver coil with the inner magnetic core.

core of the receiver coil is to reduce the influence of the magnetic field on the interior of the caput-articularis. It can't hinder the power reception. Therefore, it is located inside the

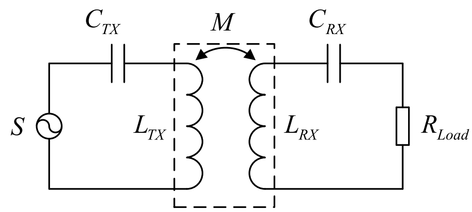

FIGURE 9. The equivalent circuit of WPT.

coil and has the same shape as the receiver coil. Fig. 8(b) shows the coils with magnetic cores.

C. THE SELF-INDUCTANCE AND MUTUAL INDUCTANCE

Fig.9 shows the equivalent circuit of WPT. The resonant frequency of the coil is adjusted by adding a compensation capacitor to the transmitter coil and the receiver coil. The transmission efficiency is maximizing when the operating frequency of the transmitter coil and the receiver coil is at or near the resonance frequency [4].

$$\eta \propto k\sqrt{Q_t Q_r} = \frac{\omega}{\sqrt{R_t R_r}} M \tag{1}$$

where η is the transmission efficiency of WPT, k is the coupling coefficient, ω is the resonance frequency, M is the mutual inductance, Q_t, Q_r, R_t and R_r are the quality factors and resistances of the transmitter coil and receiver coil, respectively.

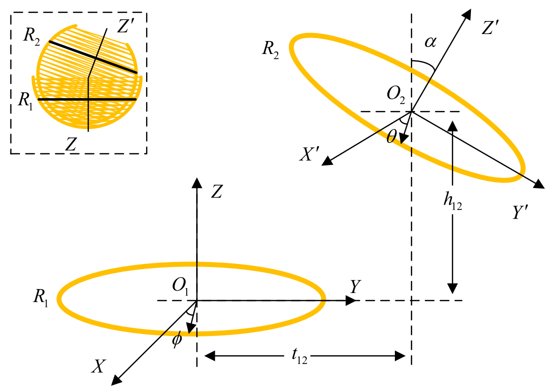

FIGURE 10. Two coils in non-coaxial and non-parallel position.

The operating frequency of the coil, that is, the output frequency of the high frequency AC source, is usually determined when the WPT is designed. To improve the transmission efficiency, the mutual inductance between the transmitter coil and the receiver coil is mainly optimized. The WPT coils in the spheroid joint are helixes with a non-linear change in diameter. They can be approximately equivalent to a series of single-turn circular coils with different diameters. When the ball-and-ball joint rotates, the position of the equivalent single coils in the transmitter coil and the receiver coil are in a non-coaxial non-parallel state, as shown in Fig. 10. According to the Neumann formula, the mutual inductance between the two coils can be obtained [19].

$$M_{12} = \frac{\mu_0}{4\pi}\int_0^{2\pi} \times \int_0^{2\pi} \frac{R_1R_2\left(\cos\theta\cos\phi + \sin\theta\sin\phi\cos\alpha\right)d\theta d\phi}{\sqrt{R'}} \quad (2)$$

where

$$R' = (R_1\cos\theta R_2\cos\phi)^2 + (R_1\sin\theta\cos\alpha + t_{12} - R_2\sin\phi)^2 + (-R_1\sin\theta\sin\phi\sin\alpha + h_{12})^2 \quad (3)$$

where μ_0 is the permeability of vacuum, R_1 and R_2 are the radii of the transmitter coil and the receiver coil respectively, and the α is the angle between the plane of the two coils, θ is the angle between the line connecting the micro-element $d\theta$ in the receiver coil and the center of the circle and the X'-axis, ϕ is the angle between the line connecting the micro-element $d\phi$ in the transmitter coil and the center of the circle and the X-axis, h_{12} and t_{12} are the vertical distance and horizontal distance between the center of the transmitter coil and the receiver coil.

For the single turn circular coil, its self-inductance can be expressed as the following expression [6].

$$L_S = \mu_0 R\left[\ln\left(\frac{8R}{r}\right) - 2\right] \quad (4)$$

where R is the radius of the single turn coil, r is the radius of the wire.

When magnetic cores are added to optimize the coils, that is the magnetic permeability of a partial magnetic circuit is improved. The mutual inductance and the self-inductance are

$$M'_{12} = \frac{\left[\delta_L + (1-\delta_L)\mu\right]\mu_0}{4\pi}\int_0^{2\pi}\int_0^{2\pi} \times \frac{R_1R_2\left(\cos\theta\cos\phi + \sin\theta\sin\phi\cos\alpha\right)d\theta d\phi}{\sqrt{R'}} \quad (5)$$

$$L'_S = \left[\delta_M + (1-\delta_M)\mu\right]\mu_0 R\left[\ln\left(\frac{8R}{r}\right) - 2\right] \quad (6)$$

where δ_L and δ_M are the ratio of the optimized path to the magnetic path.

For a coil composed of many single-turn circular coils, the self-inductance of the coil includes the self-inductance of all the single-turn coils and the mutual inductance between the single-turn coils. Hence the self-inductance of the single layer N-turn coils can be expressed as

$$L = \sum_{i=1}^{N}\sum_{j=1}^{N} M'_{ij}\begin{pmatrix} R_i, R_j, \alpha = 0, \\ t = 0, h_{ij} = |j-i|\,h' \end{pmatrix}(1-\kappa_{ij}) + \sum_{S=1}^{N} L'_S(R_S, r) \quad (7)$$

where h' is the distance between two adjacent single-turn coils, $\kappa_{ij} = 1$ when $i = j$, otherwise, $\kappa_{ij} = 0$.

Assume the angle between any single-turn circular coils in the transmitter coil and that in the receiver coil is α when the caput-articularis rotates to a certain position. The mutual inductance is

$$M = \sum_{i=1}^{N}\sum_{j=1}^{M} M'_{ij}\left(R_i, R_j, \alpha, t, h_{ij} = \left|ih' - jh''\right| + h\right) \quad (8)$$

where h' and h'' are the distance of two adjacent single turn coils in the transmitter and receiver coils respectively, and h is the distance between the transmitter coil and the receiver coil center.

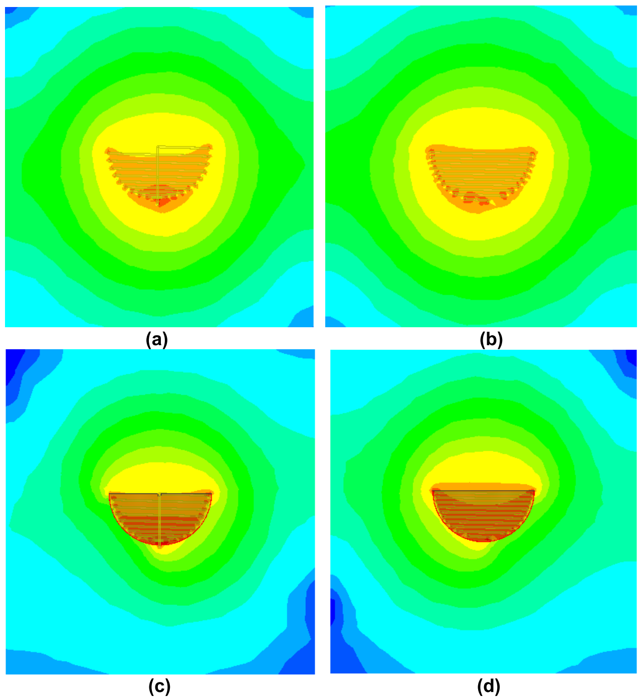

FIGURE 11. **The magnetic field distribution. (a) The transmitter coil with equal pitch between adjacent turns; (b) The transmitter coil with equal spacing between adjacent turns in vertical height; (c) The transmitter coil with equal pitch between adjacent turns added with a magnetic core; (d) The transmitter coil with equal spacing between adjacent turns in vertical height added with a magnetic core.**

III. THE OPTIMIZATION DESIGN OF SYSTEM PARAMETERS

A. THE TRANSMITTER COIL

Fig. 11 shows the magnetic field distribution of the four transmitter coils when the current of the coil is 10A. It can be seen that the magnetic field distribution can be enhanced by adding magnetic cores in the coil, and reduced outside the coil, especially under the coil. the magnetic field of the transmitter coil on the outside area of the coil is about one order of magnitude lower than that of the coil without magnetic cores. The way of adding a magnetic core gathers more magnetic fields for power transmission, and reduces the influence of the magnetic field on the surrounding environment, which is in line with the requirements put forward for the coil.

The function of the transmitter coil is to convert the electric field energy into the magnetic energy for the reception by receiver coils. In the spheroid joint, it is also necessary to ensure that the power received by the receiver coil is as stable as possible when the caput-articularis is freely rotated (that is, the receiver coil rotates). For the transmitter coil with equal pitch between adjacent turns with a magnetic core, its magnetic field is distributed in a ladder shape within the coil, and the magnetic field intensity at the bottom is much higher than that at the top. For the transmitter coil with equal spacing between adjacent turns in vertical height with a magnetic core, the distribution of the magnetic field is also similar to a ladder. However, near the inner position of the transmitter coil (that is, the position of the receiver coil), the magnetic field distribution is more uniform than that of the coil with equal pitch between adjacent turns. In other words, when the receiver coil rotates, the magnetic field distribution intensity at the position of the receiver coil changes less, and the receiver coil can receive power more stably. Hence it is more suitable for the power transmission of the spheroid joint.

TABLE 1. The parameters of the transmitter coil with a magnetic core.

Parameter	VALUE
The material of the coil	0.1*300 Litz wire
The diameter of each core line of the Lize wire	0.1mm
The number of the core lines	300
The cross section of the Lize wire	About 2.36mm^2
The outside diameter of the Lize wire	2.3mm
Pitch	5mm
Turns	10
The radius of the hemisphere	50mm
Saturation permeability of the magnetic bar	2500
The size of the magnetic bar	3*15mm

Table 1 shows the parameters of the transmitter coils with equal spacing between adjacent turns in vertical height with a magnetic core. The coil is coiled with 0.1*300 Litz wires to reduce the skin effect under high-frequency AC excitation. The magnetic core is made of many 3*15mm small magnet bars. In order to overcome the influence of the gap left during the splicing, the thickness of the magnetic core is thicker than that in the simulation design. In addition, since the magnetic core with small pieces can cut off the eddy current path, the eddy current loss will reduce. Fig. 12 shows the transmitter coil and the magnetic core.

B. THE RECEIVER COIL

Fig. 13 shows the mutual inductances between four types of receiver coils and the transmitter coil with equal spacing between adjacent turns in vertical height with a magnetic core. The distance between the transmitter coil and the receiver coil is about 5mm. Fig. 14 shows the magnetic field distribution. It can be seen that the mutual inductances between the transmitter coil and the receiver coils

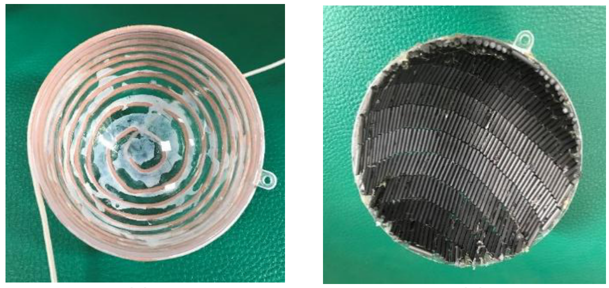

(a) (b)

FIGURE 12. The transmitter coil with equal spacing between adjacent turns in vertical height with a magnetic core. (a) The transmitter coil; (b) The magnetic core.

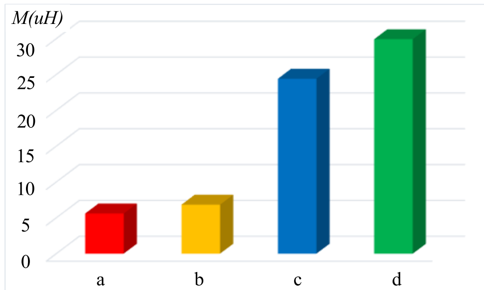

FIGURE 13. Mutual inductance. (a- The receiver coil with equal pitch between adjacent turns; b- The receiver coil with equal spacing between adjacent turns in vertical height; c- The receiver coil with equal pitch between adjacent turns added with a magnetic core; d- The receiver coil with equal spacing between adjacent turns in vertical height added with a magnetic core).

can be obviously improved by adding magnetic cores, and the magnetic cores can effectively reduce the magnetic field intensity inside the caput-articularis and the influence on the internal environment of the caput-articularis. Therefore, the receiver coil also uses a magnetic core for the structural optimization.

The receiver coil is located in the caput-articularis. It will rotate in all directions, as shown in Fig. 5. All rotations can be decomposed into horizontal rotation (with Z axis as the revolving central axis) and rotation in the vertical direction (with X axis or Y axis as the revolving central axis). In the process of rotation, the receiver coil must not only receive power, but also maintain the stability of the received power as much as possible, that is, the change of the mutual inductance between the two coils is as little as possible. Fig. 15 shows the mutual inductances of the two coils with magnetic cores when receiver coils rotates with the Z axis and the X axis as the central axis respectively. It can be seen that the mutual inductances are almost constant during the rotation in the horizontal plane. When the caput-articularis rotates in the vertical direction, the changes of the mutual inductances are the same. However, whether the caput-articularis rotates in horizontal or vertical direction, the mutual inductance between the transmitter coil and the receiver coil with equal spacing between adjacent turns in vertical height with a magnetic core (D with a magnetic core) is larger than that with

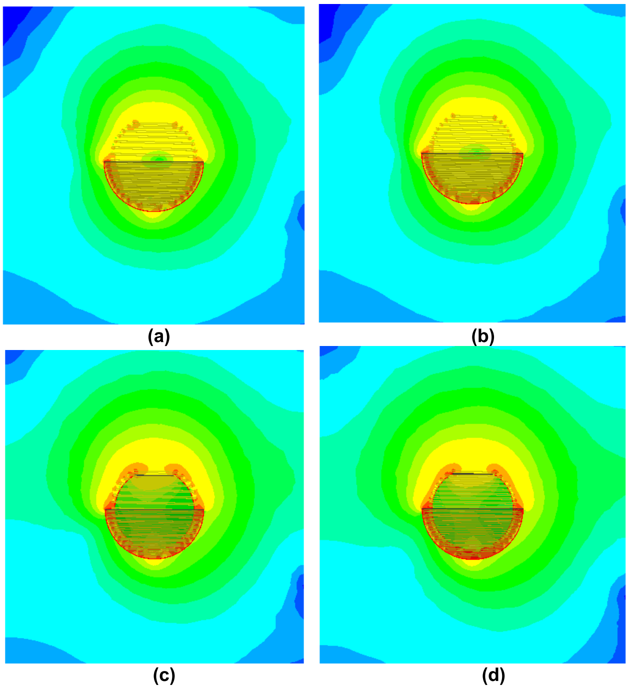

FIGURE 14. The magnetic field distribution. (a) The receiver coil with equal pitch between adjacent turns; (b) The receiver coil with equal spacing between adjacent turns in vertical height; (c) The receiver coil with equal pitch between adjacent turns added with a magnetic core; (d) The receiver coil with equal spacing between adjacent turns in vertical height added with a magnetic core.

TABLE 2. The parameters of the receiver coil with a magnetic core.

Parameter	Value
The material of the coil	The same as the transmitter coil
Pitch	5mm
Turns	18
The radius of the sphere	45mm
The parameter of the magnetic bar	The same as the transmitter

equal pitch between adjacent turns with a magnetic core. That is to say, the receiver coil with equal spacing between adjacent turns in vertical height with a magnetic core (D with a magnetic core) has higher transmission efficiency and better performance.

Table 2 shows the parameters of the receiver coil with equal spacing between adjacent turns in vertical height with a magnetic core. The wire and magnetic core material are the same as the transmitter coil. According to the design parameters, the magnetic core and the receiver coil with a magnetic core have been made as shown in Fig. 16.

IV. EXPERIMENT

The experiment platform, as shown in Fig. 17, is built to measure the transmission efficiency and transmission power of the full-freedom WPT for the spheroid joint. The DC input voltage is adjusted to change the input power. Fig. 18 shows the relationship between the transmission efficiency and the

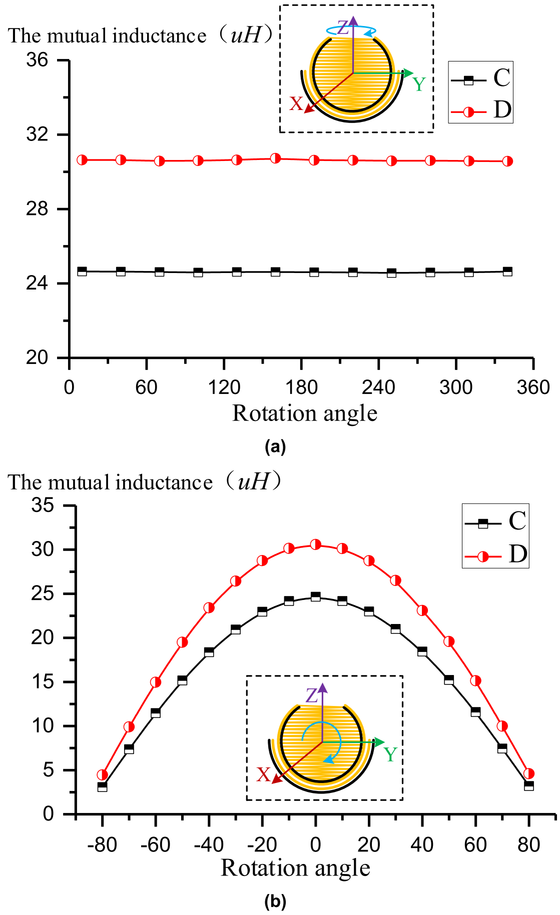

FIGURE 15. The mutual inductance between the two coils vs the rotation. (a) The Z axis as the revolving central axis. (b) The X axis as the revolving center axis.

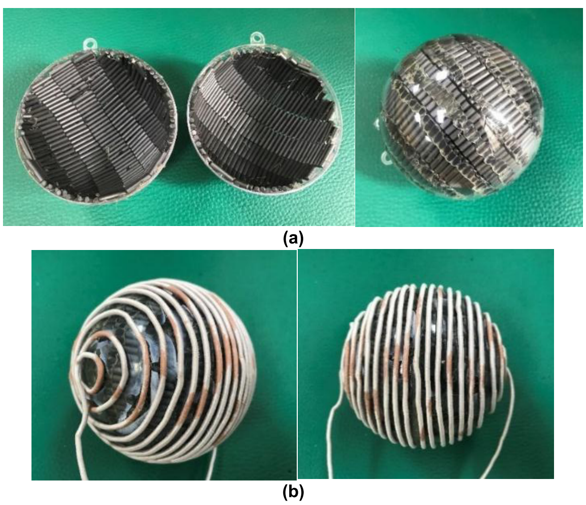

FIGURE 16. The receiver coil with equal spacing between adjacent turns in vertical height with a magnetic core. (a) The receiver coil. (b) The receiver coil with a magnetic core.

transmission power. With the increase of the DC voltage, the primary input power and the secondary receiving power rise in the same way. When the input voltage changes from

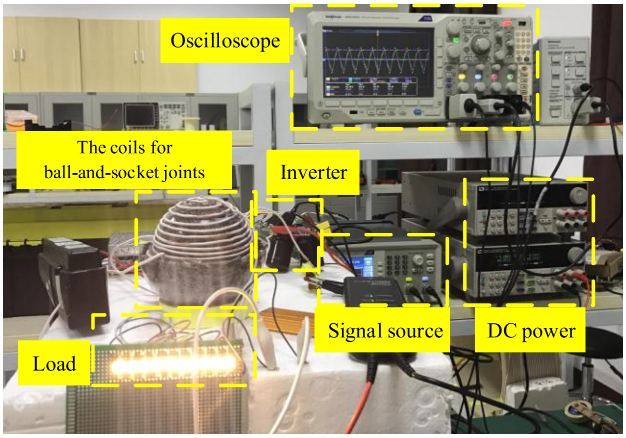

FIGURE 17. The full-freedom WPT for ball-and-socket joints.

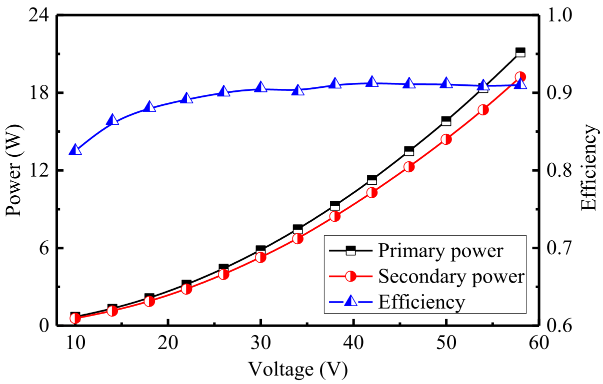

FIGURE 18. The relationship between the transmission efficiency and the transmission power.

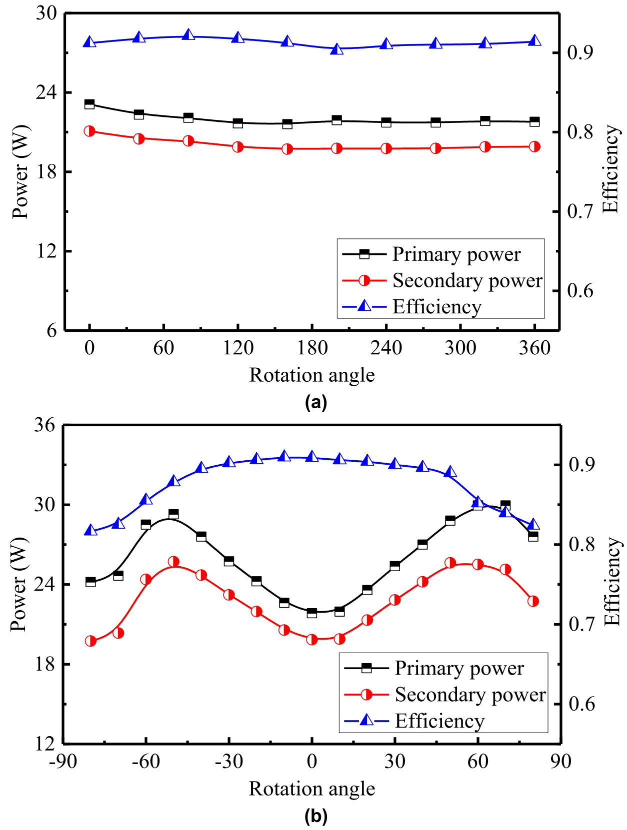

FIGURE 19. The relationship between transmission efficiency and transmission power when the ball head rotates. (a) Z axis as the central axis. (b) X axis as the central axis.

10V to 40V, the transmission efficiency of the system keeps increasing, but the increasing rate goes down. After the DC input voltage reaches 40V, the transmission efficiency is stable at around 91%. The reason is when the input power is small, the loss of the system accounts for a large proportion of the total power. When the input power grows continuously, the proportion of this part keep dropping until it becomes stable. At this time, the transmission efficiency will be constant.

According to the theoretical analysis, all movements of the spheroid joint can be divided into the combinations of rotations with the Z-axis and X-axis (or Y-axis) as the central axis. When the caput-articularis coil rotates with Z axis and X axis as the central axis, the transmission power and transmission efficiency are tested, as shown in Fig. 19.

The transmission power and transmission efficiency are almost not affected when the caput-articularis coil rotates with the Z axis as the revolving central axis, as shown in Fig. 19 (a). The transmission efficiency is about 91%. From Fig. 19(b), when the rotation angle is changed from $-80°$ to $0°$, the transmission efficiency continuously goes up. It reaches a maximum at $0°$, which is about 91.5%. But the increasing rate of the transmission efficiency keeps dropping. The transmission power enlarges during the rotation angle ranges from $-80°$ to $-50°$, and diminishes from $-50°$ to $0°$. When the rotation angle is $-50°$, it reaches the maximum. This is because, when the rotation angle changes from $-80°$ to $0°$, the mutual inductance between the two coils continuously increases, as shown in Fig. 15(b). The transmission efficiency will rise with the mutual inductance. When the rotation angle is in the range of $-80°$ and $-50°$, the WPT for spheroid joint is in deficient coupling state. The transmission power goes up with the rise of the mutual inductance. While in the interval $[-50°, 0°]$, the WPT is in the state of excess coupling. The transmission power will go down. In addition, it can also be seen that the transmission efficiency and the transmission power are symmetrically distributed in the range of the rotation angle from $-80°$ to $0°$ and from $0°$ to $80°$. The transmission efficiency is always higher than 80% when the caput-articularis rotates freely.

V. CONCLUSION

A full-freedom WPT for spheroid joint is presented in this paper. Based on the characteristics of spheroid joint, the corresponding performance requirements of coils are formulated. Through the theoretical analysis and simulation comparison, the hemispherical and spherical coils with equal spacing between adjacent turns in vertical height are selected for spheroid joint. By adding the hemispherical and spherical magnetic cores, the magnetic field distributions of the coils are optimized, and the electromagnetic effects of the external and internal environment are reduced. Finally, a corresponding experimental platform is built to verify that the transmission efficiency of the system is about 91%. The transmission efficiency with the X axis (or Y axis) as the central axis is kept above 80%. It meets the requirements that the spheroid joint can receive stable power in any state. The full-freedom WPT proposed in this paper provides a new way for the power transmission between the caput-articularis and the acetabulum in the spheroid joint.

REFERENCES

[1] A. Kurs, A. Karalis, R. Moffatt, J. D. Joannopoulos, P. Fisher, and M. Soljačič, "Wireless power transfer via strongly coupled magnetic resonances," *Science*, vol. 317, pp. 83–86, Jul. 2007.
[2] T. Arakawa *et al.*, "Optimizing wireless power transfer from multiple transmit coils," *IEEE Access*, vol. 6, pp. 23828–23838, 2018.
[3] C.-L. Yang, C.-K. Chang, S.-Y. Lee, S.-J. Chang, and L.-Y. Chiou, "Efficient four-coil wireless power transfer for deep brain stimulation," *IEEE Trans. Microw. Theory Techn.*, vol. 65, no. 7, pp. 2496–2507, Jul. 2017.
[4] Z. Dai, Z. Fang, H. Huang, Y. He, and J. Wang, "Selective omnidirectional magnetic resonant coupling wireless power transfer with multiple-receiver system," *IEEE Access*, vol. 6, pp. 19287–19294, 2018.
[5] M. Manoufali, K. Bialkowski, B. Mohammed, and A. Abbosh, "Wireless power link based on inductive coupling for brain implantable medical devices," *IEEE Antennas Wireless Propag. Lett.*, vol. 17, no. 1, pp. 160–163, Jan. 2018.
[6] Z. Dai, J. Wang, Y. Li, Y. He, Z. Fang, and H. Hou, "Optimal design of magnetic coupling wireless power supply system for monitoring equipment," *IEEE Access*, vol. 6, pp. 58600–58608, 2018.
[7] K. Lee and S. H. Chae, "Power transfer efficiency analysis of intermediate-resonator for wireless power transfer," *IEEE Trans. Power Electron.*, vol. 33, no. 3, pp. 2484–2493, Mar. 2018.
[8] S. Bandyopadhyay, V. Prasanth, P. Bauer, and J. A. Ferreira, "Multi-objective optimisation of a 1-kW wireless IPT systems for charging of electric vehicles," in *Proc. IEEE Transp. Electrific. Conf. Expo*, Jun. 2016, pp. 1–7.
[9] N. Ha-Van and C. Seo, "Analytical and experimental investigations of omnidirectional wireless power transfer using a cubic transmitter," *IEEE Trans. Ind. Electron.*, vol. 65, no. 2, pp. 1358–1366, Feb. 2018.
[10] C. Zhang, D. Lin, and S. Y. Hui, "Basic control principles of omnidirectional wireless power transfer," *IEEE Trans. Power Electron.*, vol. 31, no. 7, pp. 5215–5227, Jul. 2016.
[11] D. Wang, Y. Zhu, H. Guo, X. Zhu, T. T. Mo, and Q. Huang, "Enabling multi-angle wireless power transmission via magnetic resonant coupling," in *Proc. 7th Int. Conf. Comput. Converg. Technol.*, Dec. 2012, pp. 1395–1400.
[12] Y. Son and J.-I. Ha, "The electric variable transmission without slip ring for the hybrid electric vehicle driving structure," in *Proc. 9th Int. Conf. Power Electron. ECCE Asia*, Jun. 2015, pp. 857–862.
[13] J. Feng, Q. Li, and F. C. Lee, "Omnidirecitional wireless power transfer for portable devices," in *Proc. IEEE Appl. Power Electron. Conf. Expo.*, Mar. 2017, pp. 1675–1681.
[14] Y. Zhu *et al.*, "Comprehensive study of the flow control strategy in a wirelessly charged centrifugal microfluidic platform with two rotation axes," *Anal. Chem.*, vol. 89, no. 17, pp. 9315–9321, 2017.
[15] K. Bai, R. Xu, K.-M. Lee, W. Dai, and Y. Huang, "Design and development of a spherical motor for conformal printing of curved electronics," *IEEE Trans. Ind. Electron.*, vol. 65, no. 11, pp. 9190–9200, Nov. 2018.
[16] M. Shekarforoush *et al.*, "An explicit method for analysis of three-dimensional linear and angular velocity of a joint, with specific application to the knee joint," *J. Med. Biol. Eng.*, vol. 38, no. 2, pp. 273–283, 2018.
[17] S. Park, "Evaluation of electromagnetic exposure during 85 kHz wireless power transfer for electric vehicles," *IEEE Trans. Magn.*, vol. 54, no. 1, Jan. 2018, Art. no. 5100208.
[18] C. Xiao, D. Cheng, and K. Wei, "An LCC-C compensated wireless charging system for implantable cardiac pacemakers: Theory, experiment, and safety evaluation," *IEEE Trans. Power Electron.*, vol. 33, no. 6, pp. 4894–4905, Jun. 2018.
[19] F. Liu, Y. Yang, D. Jiang, X. Ruan, and X. Chen, "Modeling and optimization of magnetically coupled resonant wireless power transfer system with varying spatial scales," *IEEE Trans. Power Electron.*, vol. 32, no. 4, pp. 3240–3250, Apr. 2017.

ZHONGYU DAI received the B.Sc. degree from Wuhan University, in 2014, where he is currently pursuing the Ph.D. degree. His main research interests include wireless transmission technology based on magnetic resonance, applied electromagnetics, and system equipment for power transmission and distribution.

JUNHUA WANG born in Shandong, China, in 1981. He received the Ph.D. degree from The Hong Kong Polytechnic University, Hong Kong, in 2012. He joined Carnegie Mellon University as a Postdoctoral Researcher, in 2012, and then was a Research Fellow with the GATE Center for Electric Drive Transportation, MI, USA. He is currently a Professor with the School of Electrical Engineering, Wuhan University. His main research interests include wireless transmission technology based on magnetic resonance, applied electromagnetics, and system equipment for power transmission and distribution.

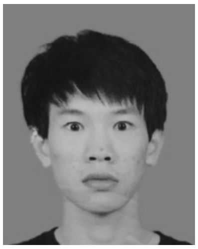

LEI JIN received the B.Eng. degree from Shanghai University, in 2017. He is currently pursuing the master's degree with Wuhan University. His main research interests include wireless power transfer and power electronics.

HANG JING received the bachelor's degree from Hunan University, in 2017. He is currently pursuing the M.E.E. degree with Wuhan University. His main research interests include wireless transmission technology based on magnetic resonance, power electronics, and applied electromagnetics.

ZHIJIAN FANG received the B.S. and Ph.D. degrees in electrical engineering and automation from the Huazhong University of Science and Technology, Wuhan, China, in 2010 and 2015, respectively.

Since 2015, he has been a Postdoctoral Research Fellow with the School of Electrical Engineering, Wuhan University, Wuhan. From 2016 to 2017, he was a Postdoctoral Research Fellow with the Department of Electrical and Computer Engineering, Ryerson University, Toronto, ON, Canada. His research interests include high-performance dc/dc converters, battery chargers, and renewable energy applications.

HAOLI HOU received the Ph.D. degree in genetics from the College of Life Sciences, Wuhan University, Wuhan, China, in 2017, where she has been a Postdoctoral Research Fellow with the School of Electrical Engineering, since 2017. Her main research interests include molecular cytogenetics, biological effect of high-frequency magnetic field, effect of low temperature on plasma, and other related research topics.